Eur. Phys. J. D **11**, 355–365 (2000)

THE EUROPEAN PHYSICAL JOURNAL D

EDP Sciences

Lifetimes of metastable states in Sr II

E. Biémont[1,2,a], J. Lidberg[3], S. Mannervik[3,b], L.-O. Norlin[4], P. Royen[5], A. Schmitt[6], W. Shi[5], and X. Tordoir[1]

[1] Physique Nucléaire Experimentale (Bât. B15), Université de Liège, Sart Tilman, 4000 Liège 1, Belgium
[2] Astrophysique et Spectroscopie, Université de Mons-Hainaut, rue de la Halle 15, 7000 Mons, Belgium
[3] Atomic Physics, Stockholm University, 104 05 Stockholm, Sweden
[4] Physics Department in Frescati, Royal Institute of Technology, 104 05 Stockholm, Sweden
[5] Physics Department, Stockholm University, P.O. Box 6730, 113 85 Stockholm, Sweden
[6] Fachbereich Physik, Universität Kaiserslautern, 67663 Kaiserslautern, Germany

Received 15 February 2000 and Received in final form 20 March 2000

Abstract. The lifetimes of the $4d\ ^2D_{3/2,5/2}$ levels of Sr^+ have been determined both experimentally and theoretically. The experiment was performed at an ion storage ring utilising collinear laser excitation. The calculation was performed by the Hartree-Fock method including relativistic effects and core polarisation. The obtained lifetimes (which are about 0.4 s) are discussed in detail and compared with earlier published results. In addition, calculated lifetimes of a large number of excited states in Sr^+ are included.

PACS. 31.10.+z Theory of electronic structure, electronic transitions, and chemical binding – 32.70.Cs Oscillator strengths, lifetimes, transition moments

1 Introduction

The singly charged strontium ion, with a single electron outside a closed shell, possesses the apparent simplicity of a one-electron system with an uncomplicated electronic structure. Accurate theoretical calculations of its properties require, however, a detailed analysis of valence and core-valence correlation and it constitutes consequently a challenge for theory.

The low-lying $4p^6 4d$ configuration of Sr^+ gives the ion attractive properties for different applications. The $^2D_{3/2,5/2}$ levels formed on this configuration are the most low-lying excited states, but since they can not decay to the ground state ($5s\ ^2S_{1/2}$) with electric dipole transitions they will stay metastable. The decay of the $4d$ levels is instead governed by electric quadrupole transitions (E2) to the ground state and the lifetimes are about 0.4 s. These long lifetimes imply extremely narrow natural line widths (0.4 Hz) of the levels. With probing technique in an ion trap, originally proposed by Dehmelt [1], the forbidden transitions could be probed and used for a very accurate optical frequency standard with a very high Q value ($\nu/\Delta\nu$). The $5s\ ^2S_{1/2}$–$4d\ ^2D_{5/2}$ transition in Sr^+ was recently selected by the Comit International des Poids et Mesures (CIPM) as a recommended optical frequency for realization of the meter [2,3]. Very recently Bernard *et al.* [4] related this transition to the Cs atomic clock by a frequency chain and they were able to determine the transition frequency with a relative accuracy better than 10^{-12}.

[a] e-mail: E.Biemont@ulg.ac.be
[b] e-mail: Mannervik@msi.se

Another area in which metastable levels have attracted interest recently is within quantum computation. Cirac and Zoller [5] have suggested that laser cooled ions in a linear ion trap could be used for quantum computing. This could be realized effectively if the excited state is metastable for which spontaneous decay is negligible. Much work has recently been devoted to studies of Ca^+ for this purpose. Since calcium is homologous to strontium, it has similar electronic structure and the singly-charged ion possesses metastable $3d$ levels with natural lifetimes of about 1 s. The linear trap set-up intended for quantum computing was recently demonstrated experimentally by Roos *et al.* [6].

Strontium, which has four stable isotopes (*i.e.* 84, 86, 87 and 88 in proportion of about 0.6, 9.9, 7.0 and 82.6%), is currently observed in astrophysics (see *e.g.* Jaschek and Jaschek [7]). Emission lines of Sr II have been identified in T Tau stars a long time ago [8]. Sr II lines are also strong in some Bp or Am stars (see *e.g.* Refs. [9,10]). Sr transitions are prominent in Ba stars [11] and are enhanced in S-type stars [12] and also in some C stars [13]. Strontium, which is also observed in the solar photospheric spectrum [14], is however underabundant with respect to iron in metal-weak stars [15]. Recently, theoretical data was used to determine strontium abundance in the HgMn-type star χ Lupi [16]. In spatially resolved studies by the Hubble Space Telescope (HST) of the star η Carinae, the forbidden $5s\ ^2S_{1/2}$–$4d\ ^2D_{3/2,5/2}$ transitions were unexpectedly observed very recently [17], an observation that can not easily be explained by astrophysical standard models. In general, the analysis of the line profiles for abundance determination in stars relies heavily upon accurate spectroscopic data (line positions and intensities).

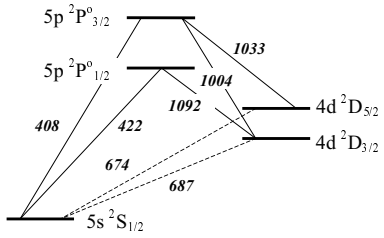

Fig. 1. Schematic level diagram of the five lowest energy levels in Sr^+. Wavelengths are given in nm.

The present work is focussed on the metastable $4d$ levels, for which we have determined the lifetimes both experimentally and theoretically. The theoretical work presented here also includes calculations for a large number of other levels.

Sr II ion shows a rather simple structure with $4p^6nl$ Rydberg states observed up to $n = 14$ (nd series) [18]. The decay of the $4d\ ^2D_{3/2,5/2}$ metastable levels to the ground level occurs *via* E2 transitions situated at 674 and 687 nm, respectively (Fig. 1). In two recent experiments (Gerz *et al.* 1987 [19]; Madej and Sankey [20]), Sr^+ ions were stored in radio-frequency quadrupole traps and the lifetimes of the $^2D_{3/2,5/2}$ states were measured using laser excitation. Some discrepancies between these measurements and the few available theoretical lifetimes available in the literature were observed.

Accurate calculations of atomic structures in a "heavy" ion like Sr II are very difficult and require that both configuration interaction and relativistic effects are taken into account. In order to limit the number of configurations that should be included explicitly in the calculations by opening the inner shells, core polarisation effects can be incorporated in the physical model in a semi-empirical way but the adopted model requires accurate experimental data in order to be tested. In this paper we provide both accurate measurements of the $4d$ metastable levels and theoretical calculations of the lifetimes of these levels as well as of additional levels (up to $n = 10$) of Sr II.

Up to now, experimental lifetime measurements in the Sr^+ ion are rather sparse and concern only 6 different levels. They have been obtained by the Hanle-effect technique [21–23], by fast-beam-laser measurements [24,25] and finally by the use of radio-frequency traps [19,20]. Theoretical results have been obtained for the metastable $4d\ ^2D$ states by Guet and Johnson [26] in the framework of the Many Body Perturbation Theory (MBPT), by Warner [27] using a Scaled Thomas-Fermi approximation and by Poirier [28], who used a semi-empirical method. The discrepancies between the different sets of results and the lack of data for some levels call for a new detailed theoretical determination of transition probabilities in Sr II.

The experimental results in this work were obtained by the techniques recently developed for lifetime measurements in ion storage rings. These methods were most recently successfully applied to the metastable $3d$ levels in Ca^+ [29].

2 Calculations

2.1 Method

We have used for the present calculation the relativistic Hartree-Fock (HFR) method *i.e.* a Hartree-Fock method including relativistic corrections to the wavefunctions [30,31]. The Slater parameters are computed *ab initio* and the energies and spectra are obtained in intermediate coupling with HFR basis functions using the Slater-Condon theory. This approach is based on the non-relativistic Schrödinger equation but considers the most important relativistic effects such as the mass-velocity terms and the Darwin correction.

A set of 46 configurations has been retained for the final calculations, the limits being imposed by the computer space available. In the present work, intravalence correlation is introduced by considering the Rydberg series up to $n = 12$. The following configurations outside of the core $3d^{10}4s^2$ have been retained in the model:

$$4p^6ns\ (n = 5{-}12) + 4p^6nd\ (n = 4{-}12) + 4p^55s5p + 4p^55s6p + 4p^55s4f + 4p^55s5f + 4p^55s6f$$

and

$$4p^6np\ (n = 5{-}12) + 4p^6nf\ (n = 4{-}12) + 4p^55s6s + 4p^55s4d + 4p^55s5d + 4p^55s6d + 4p^55s^2 + 4p^56s^2 + 4p^55p^2.$$

In order to improve the agreement between calculated eigenvalues of the Hamiltonian and the observed energy levels (when available), a well established least-squares-fitting procedure has been used, the Slater integrals F^k, G^k and R^k and spin-orbit integrals being considered as adjustable parameters. All the available experimental levels (up to $n = 12$) have been included in the calculations. They were taken from Moore [18], since the more recent analysis of Newsom *et al.* [32] only contains wavelengths and not levels. The parameter values used for the calculations are given in Table 1. Only the Slater parameters and spin-orbit integrals of the configurations for which experimental energy levels exist are reproduced in the table. Configuration interaction parameters, which were left at their *ab initio* values are not quoted in the table.

2.2 Polarization effects

Polarization effects are expected to be important in Sr II. They have been analyzed recently by Migdalek and Baylis [33]. In the present context, the core polarisability, α_p, in the potential $V_p(r)$ has been set equal to the static dipole polarisability calculated for the bare ion with $4p^5$ configuration in the core. This procedure has been used with success previously in many heavy ions like *e.g.* Yb II [34] or Fr I [35]. It has been obtained through variational perturbation calculations by Fraga *et al.* [36] (Hartree-Fock wavefunctions). In Sr II, the α value (in a_0^3 units) is $4.926a_0^3$ or 0.73 Å^3 [36]. The cut-off parameter r_0 was

Table 1. Sr II: average energies and spin-orbit integrals (in cm^{-1}) used in the calculations.

Configuration	Parameter	Value	Configuration	Parameter	Value
$5s$	E_{av}	0	$5p$	E_{av}	23494
$6s$	E_{av}	47430		ς_{5p}	426
$7s$	E_{av}	64384	$6p$	E_{av}	55388
$8s$	E_{av}	72550		ς_{6p}	150
$9s$	E_{av}	77123	$7p$	E_{av}	68090
$10s$	E_{av}	79942		ς_{7p}	72
$11s$	E_{av}	81803	$8p$	E_{av}	74576
$12s$	E_{av}	83095		ς_{8p}	40
$4d$	E_{av}	14214	$9p$	E_{av}	78350
	ς_{4d}	150		ς_{9p}	25
$5d$	E_{av}	52951	$10p$	E_{av}	80741
	ς_{5d}	32		ς_{10p}	16
$6d$	E_{av}	66934	$11p$	E_{av}	82354
	ς_{6d}	14		ς_{11p}	11
$7d$	E_{av}	73933	$12p$	E_{av}	83491
	ς_{7d}	7		ς_{12p}	8
$8d$	E_{av}	77956	$4f$	E_{av}	60129
	ς_{8d}	5		ς_{4f}	0
$9d$	E_{av}	80482	$5f$	E_{av}	70236
	ς_{9d}	3		ς_{5f}	0
$10d$	E_{av}	82174	$6f$	E_{av}	75739
	ς_{10d}	2		ς_{6f}	0
$11d$	E_{av}	83360	$7f$	E_{av}	79053
	ς_{11d}	1		ς_{7f}	0
$12d$	E_{av}	84226	$8f$	E_{av}	81200
	ς_{12d}	1		ς_{8f}	0
			$9f$	E_{av}	82670
				ς_{9f}	0
			$10f$	E_{av}	83718
				ς_{10f}	0
			$11f$	E_{av}	84491
				ς_{11f}	0
			$12f$	E_{av}	85081
				ς_{12f}	0

calculated by [33] and was adjusted for each (nlj) state to match experimental ionisation energies. The result obtained is 1.565 Å, which is close to the value $\langle r_c \rangle = 1.498$ calculated by the HFR code for the outermost orbital of the $4s^2 4p^5$ configuration of Sr IV. The calculated lifetimes are reported in Table 2.

3 Experimental

3.1 General

The radiative decay of metastable states is difficult to study due to the long lifetimes (often milliseconds or seconds) and consequently long observation times are required. Furthermore, the atom or ion has to be prevented from non-radiative decay caused by collisions or external fields. The development of traps for ions and atoms opened the possibilities for such measurements, since long trapping times were achieved and the vacuum conditions were good. One early example of such a measurement is the determination of the long lifetime (59 s) of the $2s\ ^3S$ in Li^+ [37]. About ten years later ion storage rings intended for atomic studies were started. These devices opened alternative techniques for studies of metastable states (see *e.g.* [38–40]). We have developed techniques based on laser methods, which will be described in the following sections.

3.2 Laser probing

Laser probing as a method for lifetime studies of fast ions was introduced at the CRYRING ion storage ring about five years ago. In a first experiment the method was used for hyperfine resolved studies of metastable states in Xe^+ [41]. Utilizing the inherent high spectral resolution of the method, a remarkable strong hyperfine induced quenching was observed for one hyperfine state. The method has subsequently been developed further and it has been shown that accuracies of a few percent could be reached for lifetimes between 50 ms and 1 s. The probing method has been described in detail in reference [42] and will only briefly be presented here.

The present experiment was performed at the ion storage ring CRYRING [43] at the Manne Siegbahn Laboratory in Stockholm. An electron impact ion source (MINIS)

Table 2. Sr II: radiative lifetimes.

Level	Energy[#] (cm^{-1})	This work HFR	This work EXP	Previous
$6s\ ^2S_{1/2}$	47737	4.97		
$7s\ ^2S_{1/2}$	64964	7.32		
$8s\ ^2S_{1/2}$	73237	11.76		
$9s\ ^2S_{1/2}$	77858	18.41		
$10s\ ^2S_{1/2}$	80702	22.44		
$4d\ ^2D_{3/2}$	14556	422 ms	435±4 (455±29) ms	395±38[a] ms, 454[c], 257[i], 441[q]
$4d\ ^2D_{5/2}$	14836	384 ms	408±22 ms	345±33[a] ms, 372±25[f], 405[c], 209[i], 396[q]
$5d\ ^2D_{3/2}$	53286	3.62		
$5d\ ^2D_{5/2}$	53373	3.85		
$6d\ ^2D_{3/2}$	67523	6.60		
$6d\ ^2D_{5/2}$	67563	6.90		
$7d\ ^2D_{3/2}$	74621	11.28		
$7d\ ^2D_{5/2}$	74643	11.70		
$8d\ ^2D_{3/2}$	78689	18.15		
$8d\ ^2D_{5/2}$	78702	18.72		
$9d\ ^2D_{3/2}$	81240	24.91		
$9d\ ^2D_{5/2}$	[81249]	25.58		
$10d\ ^2D_{3/2}$	82952	33.70		
$10d\ ^2D_{5/2}$	82954	34.53		
$5p\ ^2P^0_{1/2}$	23715	7.71		6.74±0.20[b], 7.39±0.07[d], 7.35±0.30[k,p], 7.47±0.07[e], 7.48[c], 7.5[m], 6.4[n], 7.43[q]
$5p\ ^2P^0_{3/2}$	24517	6.96		5.63±0.17[g], 6.69±0.07[e],6.63±0.07[d], 6.53±0.20[k,p], 6.64±0.19[j], 6.74[c], 6.8[m], 6.4[n], 6.70[q]
$6p\ ^2P^0_{1/2}$	55770	37.50		
$6p\ ^2P^0_{3/2}$	56058	33.80		
$7p\ ^2P^0_{1/2}$	68645	96.41		
$7p\ ^2P^0_{3/2}$	68794	88.55		
$8p\ ^2P^0_{1/2}$	-	178.3		
$8p\ ^2P^0_{3/2}$	75312	170.6		
$9p\ ^2P^0_{1/2}$	-	446.3		
$9p\ ^2P^0_{3/2}$	-	441.9		
$10p\ ^2P^0_{1/2}$	-	651.1		
$10p\ ^2P^0_{3/2}$	-	648.7		
$4f\ ^2F^0_{5/2}$	60992	3.17		3.09±0.06[d], 3.3[m], 2.8[n]
$4f\ ^2F^0_{7/2}$	60992	3.23		2.97±0.05[d], 3.3[m], 2.8[n]
$5f\ ^2F^0_{5/2}$	71066	5.25		
$5f\ ^2F^0_{7/2}$	71066	5.33		
$6f\ ^2F^0_{5/2}$	76553	8.41		
$6f\ ^2F^0_{7/2}$	76553	8.52		
$7f\ ^2F^0_{5/2}$	79861	12.70		
$7f\ ^2F^0_{7/2}$	79861	12.85		
$8f\ ^2F^0_{5/2}$	82006	18.46		
$8f\ ^2F^0_{7/2}$	82006	18.67		
$9f\ ^2F^0_{5/2}$	83473	25.83		
$9f\ ^2F^0_{7/2}$	83473	26.11		
$10f\ ^2F^0_{5/2}$	84521	34.92		
$10f\ ^2F^0_{7/2}$	84521	35.31		

HFR: theoretical result, relativistic Hartree-Fock, EXP: experimental results. * Expressed in *ns* except when otherwise indicated. [#] From Moore (1958) [18]. [a] Gerz *et al.* (1987) (ion trap and laser excitation) [19]. [b] Kelly *et al.* (1974a) (Hanle effect) [22]. [c] Guet and Johnson (1991) (Many Body Perturbation Theory) [26]. [d] Pinnington *et al.* (1995) (fast-beam-laser measurement) [25]. [e] Kuske *et al.* (1978) (fast-beam-laser measurement) [24]. [f] Madej and Sankey (1990) (ion trap and laser excitation) [20]. [g] Kelly *et al.* (1974) (Hanle effect) [23]. [i] Warner (1968) (Scaled Thomas-Fermi method) [27]. [j] Rambow and Schearer (1976) (Hanle effect) [21]. [k] Smith and Gallagher (1966) [54]. [m] Pinnington *et al.* (1995) (Coulomb approximation) [25]. [n] Lindgard and Nielsen (1977) (Coulomb approximation) [55]. [p] Gallagher (1967) [56]. [q] Poirier (1993) [28].

was used to produce Sr^+ ions. The ions were accelerated to 40 keV and by 90° bending magnet the isotope of mass 88 was selected. The ions were injected and about 10^9–10^{10} could be stored in the storage ring at this beam energy. It has been found that a certain fraction of the ions extracted from the ion source are in the metastable states. The magnitude of this fraction is hard to determine but it has been estimated to be of the order 0.1–1%, depending on the actual conditions in the ion source.

In the probing method, the decay of the *metastables produced in the ion source* has been studied. These ions will decay spontaneously while being stored in the ring. Photons emitted from this spontaneous decay process will be distributed all over the ring and the efficiency for passive photon detection would be very low at a storage ring with 51.6 m circumference. For a metastable fraction as low as that obtained from the MINIS source, such detection would be impossible. The probing method on the other hand, takes advantage of the possibility to excite the metastable state to a *higher* state and to observe the prompt fluorescence from the decay of that state. In the case of Sr^+, excitation of the $4d$ levels to the $5p$ levels could be achieved by a 1 μm laser and fluorescence of the prompt decay (at about 400 nm) of the $5p$ levels to the ground state ($5s$) can be observed (see Fig. 1). The advantage here is that fluorescence could be induced and localized in front of a single detector and very high detection efficiency is obtained. The intensity of the fluorescence induced by the laser probe pulse gives a measure of the metastable population at the particular time when the laser is applied. With synchronization of the laser pulse to the control system of the ring, the decay process could be studied. Lifetime curves are recorded by a sequential variation from ring cycle to ring cycle of the delay time between ion injection into the ring and the laser pulse [42].

The wavelengths around 1 μm were produced by a standing-wave Ti:sapphire laser, SpectraPhysics model 3900. Fluorescence light was detected by a cooled photomultiplier (PM) equipped with a colored glass filter. The laser used in this experiment was not actively stabilized as was the one used in the calcium experiment [29,42]. Since the decay curve is built up sequentially with one time point for each ring cycle, the lower stability of the laser caused a larger scatter between data points than what would be anticipated from pure statistical considerations. Besides the different laser system, the same equipment and the same procedure were used as for the calcium experiment [29,42] and we refer to these articles for further details.

3.3 Optical pumping

Although the detection efficiency, as well as the signal-to-background ratio, is very high for the laser probing this method has some drawback. Firstly, the sequential build-up of the decay curve may give rise to systematical errors. To avoid such errors different normalization and correction curves have to be recorded. Secondly, since the metastable ions produced in the source are used for the lifetime studies, the measurement must start at times as soon as possible after ion injection. It has, however, been found that ion losses occur just after injection, which must be considered in the lifetime analysis. A method to cure both these problems would be to populate a large fraction of the beam in the metastable state some time after the beam has been stored. With such a method, effects from the initial non-exponential beam loss right after injection could be avoided and if the populated fraction is large ($> 10\%$), passive detection of the radiative decay would be feasible even with a single PM tube. The latter fact gives the opportunity to record the whole decay curve by a multiscaling technique for every cycle. These considerations motivated us to also try such a method. This was done by transferring ground state ions to the metastable $4d\ ^2D_{3/2}$ level by *optical pumping*. This experiment was recently described in a separate letter [44] and here only a brief description will be given.

After injection of ions into the ring, blue laser light (422 nm) was applied to the stored ion beam in order to excite the $5s\ ^2S_{1/2}$ level to $5p\ ^2P^0_{1/2}$. The upper state will either decay back to the ground state (95%) or to the metastable $4d\ ^2D_{3/2}$ state (5%). With the excitation-deexcitation cycle repeated a number of times, the ground state ions will be transferred to the metastable state. The fraction of ions in the metastable state in the beam could be estimated from the reduction of the laser-induced fluorescence at 422 nm and the final relative population was found to be higher than 70%. With this high population of the metastable level, repopulation through collisional excitation of the ground state ions gives no significant contribution [44]. For the low metastable fraction present in the ion beam directly from the source, repopulation gives a small but significant contribution [42,45]. This contribution should be recorded and corrected for [42], as was done for Ca^+ [29] as well as in the present work on Sr^+ when the laser probing technique was used.

Laser light at 422 nm was generated by extra-cavity frequency doubling [44] of infrared laser light from a Coherent 899-29 ring Ti:sapphire laser with Autoscan pumped by an Innova 400-25 argon ion laser. At most 4 mW of blue laser power was generated in this way. After losses in optical elements and beam transport, the ion beam was typically exposed to a laser power of about 1 mW. As was reported in reference [44], the measurement with this technique was very successful and the error bar for the recorded lifetime was as small as 1%. The frequency doubling was obtained by a quasi phase-matched periodically poled KTP crystal [46], specially tailored for this experiment [44]. No crystal was available for excitation of the other transition $5s\ ^2S_{1/2}$–$5p\ ^2P^0_{3/2}$ at 408 nm, which would be required to pump the other metastable level $3d\ ^2D_{5/2}$. Optical pumping of this level is, however, more complicated, since the $5p\ ^2P^0_{3/2}$ can decay to both metastable levels. For selective population of only the $3d\ ^2D_{5/2}$ level, a second infrared pump laser would be needed.

3.4 Ion beam properties and collisional quenching

The intensity of the injected ion beam gave a number of stored ions close to the maximum that could be stored in the ring. A current transformer was used to measure the intensity of the beam during the ring cycle. In the present case the beam current was 1–4 μA. The intensity decay of the stored ions could also more accurately be measured with a neutral particle detector placed after one of the bending magnet. This detector consists of a BaF_2 scintillator and a PM tube [42,47]. At high beam intensity, there is always a strong initial peak of ion beam current, which vanishes in a few tenths of a second. The intensity of this peak appears to be dependent of the injected ion beam intensity and we interpret the effect to be due to space charge effects and beam optical effects related to the injection.

The size of the stored ion beam is large for the ions stored at injection energy. The beam diameter was about 40 mm. The velocity spread of the stored ions gave a Doppler width just below 300 MHz (FWHM) for excitation at 408 nm. The diameter of the laser beam was about 10 mm.

The lifetime of the ion beam is mainly determined by the cross-section for neutralization of the ions in collisions with the residual gas in the vacuum system. The rest gas pressure was so low that it could not be measured on an absolute scale by vacuum gauges, but it was estimated to be below 10^{-11} mbar, with H_2 as the main component ($> 90\%$) of the residual. At the lowest vacuum pressure the lifetime of the stored Sr^+ beam was found to be 64 s, corresponding to a neutralization rate of 0.016 s^{-1} (*i.e.* for the ground state ions). The metastable states in Sr^+ could also be lost by collisions with the residual gas. This loss could be neutralization (for which the cross-section, in principle, might be different from that of the ground state) but also deexcitation without charge change (Penning effects). The collisional loss was investigated by raising the rest gas pressure and recording the lifetime of the metastables at different pressures [29,42,44]. This measurement could be done accurately in the strontium measurement with optical pumping and it was found that the loss rate of the metastable state at base pressure was 0.1 s^{-1}. The results from these measurements were used for correction of the values obtained by the laser probing technique also.

4 Results

As described above, two different methods were used for the lifetime measurements in Sr^+. In a first run in April 1998, the laser probing technique was utilized and in a run in February 1999 optical pumping was used, which was briefly discussed with emphasis on the novel experimental technique in a previous letter [44]. This latter experiment was useful to support of the first measurement. The different runs will here be discussed in one context.

A typical curve from laser probing is shown in Figure 2. The fluorescence intensity was strong and yielded high

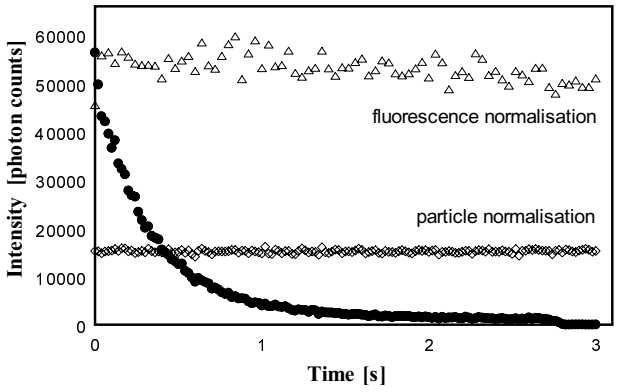

Fig. 2. Lifetime curve of the $4d\ ^2D_{3/2}$ level in Sr^+ measured by the laser probing technique. The two different normalisation curves are also given in the figure. The upper curve shows the signal monitoring the number of injected metastable ions as obtained by intermittent probing pulses at a fixed delay time. The particle curve monitors the total number of stored particles in every pulse. The kink at the end of the decay curve corresponds to the ion beam dump.

statistics. A lifetime curve as the one in the figure required about one hour data collection time and the counts in every time-point on the curve were accumulated during four ring cycles (obtained by scanning over the decay curve four times). For all curves recorded by the probing technique, the scattering between the points was larger than expected from pure statistics. For every decay curve, two different normalization curves were recorded: one curve monitored the intensity of stored ions (by recording particles), the other monitoring the number of injected metastable ions (by recording fluorescence), as described previously [29,42]. Since the scattering in the fluorescence curves (decay and normalization) was larger than in the particle curve, we conclude that the large scattering is related to instabilities in the laser frequency delivered by the laser, which was lacking active stabilization. In between the recording of the decay curves, repopulation of the metastable levels by collisional excitation was determined [29,42] (see Fig. 3), also with simultaneous recording of the two types of normalization curves. The repopulation curve was corrected by the normalization curves and then subtracted from the corresponding decay curve. Thus a decay curve (a pure single exponential decay) was obtained reflecting the decay of the metastable ions extracted from the ion source. This decay rate was, however, the sum of the natural radiative decay and other loss mechanisms (neutralization, collisional deexcitation, other losses in the storage ring due to beam optical effects). The strength of these loss mechanisms had to be determined in order to deduce the lifetime for radiative decay.

Measurements of the stored ion beam by the particle detector [42] give information about the loss of ions during the storage time. At the low energy used here, the major loss is by neutralization of the ions and since the major fraction was ions in the ground state, the lifetime mainly reflected the cross-section for neutralization of ground

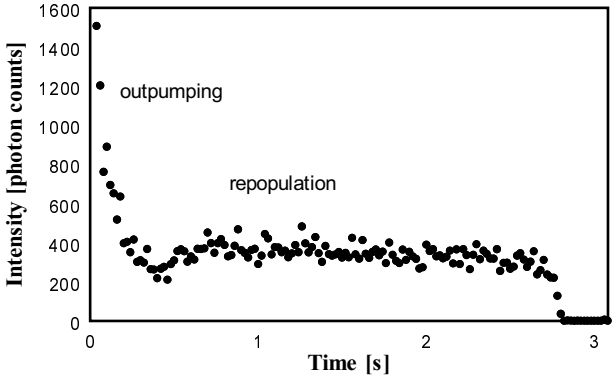

Fig. 3. Measurement of the collisional excitation of the $4d\ ^2D_{3/2}$ level in Sr^+. The first part of the curve is due to outpumping of the metastable levels populated in the ion source by use of a prompt laser pulse. This pulse lasted 0.5 s and after this time the collisional excitation is probed by a second probe pulse applied at variable delay time.

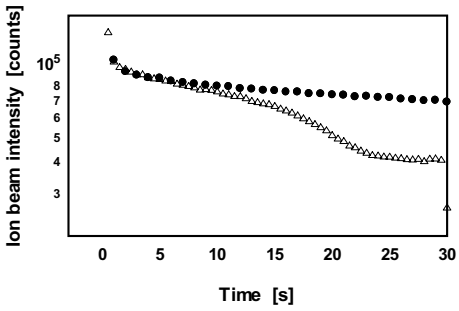

Fig. 4. Decay of the stored ion beam intensity. Filled circles correspond to the run performed in February 1999, while the open triangles correspond to the previous run in April 1998. For the first 12 s, the April run has a steeper decay (by a factor of 2.5), which is presumably mainly due to higher base pressure. The kink after 15 s is due to an instrumental effect in the storage ring during this particular run, an effect that did not influence the lifetime measurements during the first 3 seconds.

state ions. There are also clear indications that there are additional losses related to the beam intensity and the setting of beam parameters for the ring. In the case of Sr^+, for which the lifetime is about 0.4 s, the length of the ring cycle was chosen to be 3 s. Some curves for much longer cycle time were, however, also recorded in order to determine the neutralization rate accurately. In Figure 4 two different ion beam current intensity curves are given, one from the April 1998 run and one from February 1999. The latter was recorded for 60 s (although only the first 30 s is shown) and was straight lined in the logarithmic plot until the end of the cycle and the lifetime of 64 ± 1 s was found. As can be seen from Figure 4, the slope of the 1998 run is steeper than the 1999 run in the straight part before 15 s. We obtained a lifetime of 26 ± 1 s here. This could indicate that the vacuum is 2.5 times better in the later run, but since vacuum is too low to be measured by vacuum gauges this can not be confirmed. Other experiment indicate that the vacuum had been improved,

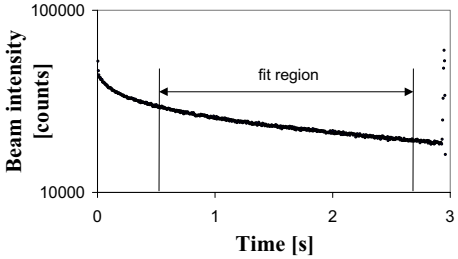

Fig. 5. The ion beam intensity decay recorded with the particle detector simultaneously with a fluorescence decay curve of the $4d\ ^2D_{3/2}$ level in Sr^+. The region used for fitting the fluorescence decay is indicated (0.5–2.7 s). As can be seen in the figure, there is a remaining small curvature from the initial fast decay, which was compensated for (as mentioned in the text). The start time for the lifetime fits was varied between 0.5 and 1.0 s to investigate systematical effects.

but without any quantitative measure. It is not possible to certify that the shorter lifetime is entirely due to higher residual pressure or if there are also some contributions from beam optical effects.

In the beginning of each cycle there is a strong peak which falls off quickly as can be seen in Figures 4 and 5. We have found that the intensity of this first transient peak is related to the intensity of the ion beam. For low intensities the transient peak is weak and we conclude that space charge effects somehow causes this fast decay. This fast decay causes problems for the lifetime measurements of the metastable lifetimes by probing. Since these measurements are made on ions produced in the ion source, it is desirable to start analysis as close as possible to injection where the metastable fraction is highest. For an early analysis, the fast initial beam loss must be disentangled. The repopulation curves recorded for Sr^+ required, however, a laser quenching pulse of 0.5 s [42], which implied that analysis could not be started until after 0.5 s. At this time most of the fast transient decay has gone but a small effect is still left as can be seen in Figure 5. This effect was compensated for in the final analysis in the following way. The slope of the particle curve in the time region 1–2.7 s was determined. This was steeper than for the main decay component of 26 s. It is plausible that this extra contribution is due to intra-beam scattering and beam optical effects and that it consequently should be the same for both ground state ions and metastable ion. Thus this extra contribution to the slope has been subtracted from the observed decay rate of the metastable levels when the radiative decay should be extracted ("Correction for beam loss" in Tab. 3). The fluorescence decay curves, corrected for repopulation, were fitted by a single exponential and background. The fitting interval was varied to find a lifetime value independent of start time. Usually fitting could be started from 0.7 s.

The correction for collisional loss, on the other hand, will be dependent on whether the ion is excited or not. In the work on Ca^+ [29], the total cross-section for neutralization and quenching of the metastable levels was estimated to be 3.8 times higher than the cross-section for neutralization of the ground state at the beam

Table 3. Experimental lifetime values for the metastable $4d\ ^2$D levels in Sr^+. The table summarizes all corrections and error estimates made to obtain the final experimental values. The column containing "measured lifetimes" gives the lifetime value with statistical error from the fit of the raw data corrected for repopulation (in the case of laser probing). Next column gives corresponding values expressed as rates and within parentheses the additional error estimate for the repopulation correction is given. Both these errors and the uncertainties given in the following two columns are summed in quadrature to yield the total uncertainty for the radiative decay rate.

Level	Method	Measured lifetime [ms]	Measured rate [s^{-1}]	Correction for beam loss [s^{-1}]	Collisional loss [s^{-1}]	Radiative decay rate [s^{-1}]	Radiative lifetime [ms]
$4d\ ^2D_{5/2}$	Laser probing	345 ± 10	2.895 ± 0.085 (± 0.088)	−0.212 ± 0.042	−0.232 ± 0.030	2.451 ± 0.133	408 ± 22
$4d\ ^2D_{3/2}$	Laser probing	379 ± 15	2.640 ± 0.107 (± 0.080)	−0.212 ± 0.042	−0.232 ± 0.030	2.196 ± 0.143	455 ± 29
$4d\ ^2D_{3/2}$	Optical pumping	416 ± 3	2.404 ± 0.017	0	−0.104 ± 0.011	2.300 ± 0.020	435 ± 4

energy of 40 keV. This result was obtained by studies at raised base pressure in the storage ring. The same method was applied for laser probing of strontium. Here, however, the measurements were not conclusive due to less stable conditions, in particular regarding the laser stability. In the experiment utilizing optical pumping, the measurements at different base pressures gave, on the other hand, very conclusive results [44]. In Figure 6a the decay of the metastable levels and the ground state ion beam, respectively, are compared. The slope of the line for the metastable level is 6.1 ± 0.8 times larger than for the ground state, which then corresponds to the ratio between the cross-section for collisional quenching (neutralization and collisional deexcitation) of the metastable ions and the neutralization cross-section for ground state ions. This ratio was used to estimate the contribution from collisional quenching also in the laser probing measurements.

The results from the measurement by optical pumping have already been published [44] and will only briefly be commented here. In this experiment no correction for repopulation was needed. Repopulation is caused by collisional excitation by the residual gas. The total strength of this process is here even lower than for the laser probing measurements, since only a small fraction of the ions are in the ground state. This fact also manifests itself in the lack of a tail on the decay curve. The decay curve (Fig. 7) comes down to pure detector background at the end of the curve and the ion beam dump is not even observed. For the probing measurement, the repopulation correction of the lifetime is of the order of 10%. In the optical pumping experiment, the metastable population was increased by orders of magnitude (presumably by at least a factor of 1000) implying that influence from repopulation is negligible at the present level of accuracy.

Optical pumping was applied 0.275 s after injection and was maintained for 1.55 s. Consequently, the lifetime analysis could not start until pumping had been switched off (*i.e.* 1.825 s after injection) and here we assume that no remaining contribution from the fast prompt beam loss is present. Nine different measurements gave results within expected statistical error bars. The only remaining effect to compensate for is collisional loss. This was done by extrapolating a Stern-Vollmer plot to zero pressure (Fig. 6b). The problem here was that pressure could not be measured. Stable raised pressure was obtained by heating a NEG pump in one of the twelve sections of the ring [42].

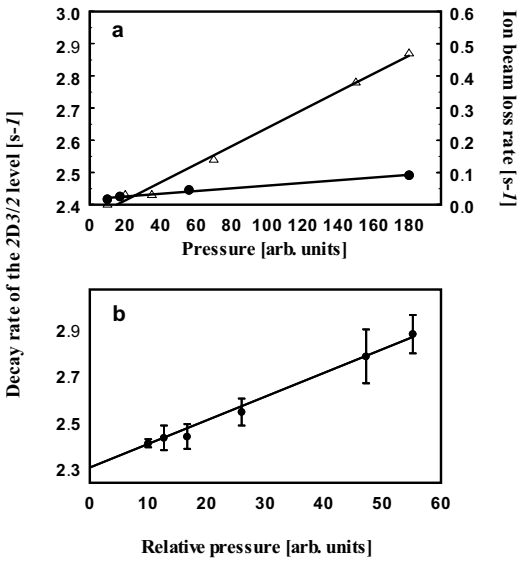

Fig. 6. Investigation of collisional quenching of the the metastable levels and of the neutralization of the ion beam by variation of the residual gas pressure. In (a) the loss rate *versus* pressure is shown both for the metastable levels (left hand scale, △) and of the stored ion beam (right hand scale, •). The slopes differ by a factor of 6.1. The pressure scale is proportional to the reading of the vacuum meter in the ring section where the pressure was raised. In (b) a Stern-Vollmer plot is obtained by using the measured decay constant of the stored ion beam to obtain a correct relative pressure scale in order to obtain the intercept of the line at the ordinate. Extrapolation of the data to the intercept yields the decay rate without contribution from collisional quenching.

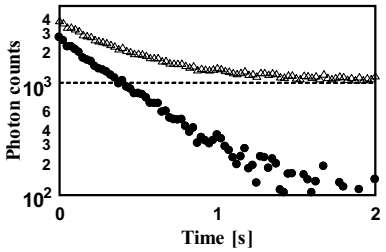

Fig. 7. Spontaneous radiative decay of $4d\ ^2D_{3/2}$ level in Sr^+ as measured by optical pumping. The dashed line indicates the detector background level. With the background level subtracted, a single exponential decay curve is observed.

The local pressure could then be directly measured by a vacuum gauge close by (this local pressure is given for the abscissa in Fig. 6a), but the average pressure experienced by the beam for one round trip in the ring could not be determined. The lifetime of the stored ion beam intensity is, however, proportional to the average pressure and thereby we could achieve the relative pressure increase from base pressure accurately. The intercept at zero pressure in the Stern-Vollmer plot is not dependent on the absolute pressure values on the abscissa but only on the relative values. By measurements of the kinetic energy loss of a stored deuteron beam, it has been concluded that the base pressure is about 10 ptorr [48]. The correction for collisional loss was by this method found to be 4% at base pressure.

The metastable lifetimes obtained by laser probing are given in Table 3. Here the contributions from different corrections are given explicitly with estimated error bars. The repopulation correction changes the shape of the curve and contributions from this correction can consequently not be expressed as an absolute number. We have, however, forced a single exponential fit to the decay curve without repopulation correction to get an idea of the influence of this correction and we have then obtained relative change of typically 10%. From correction with different repopulation curves we have tried to estimate the uncertainty here. A conservative estimate here is 3% (*i.e.* 30% uncertainty in the correction contribution). This large uncertainty is due to the large scattering between points in the raw data points discussed above, which did not allow very accurate fitting functions for the repopulation. The error bars of the four different sources of uncertainty are summed quadratically to yield the final uncertainty.

For the $4d\ ^2D_{3/2}$ level, for which have determined the lifetime with two different methods, the value obtained with laser probing is slightly longer, though within error bars. It should be noted that if the beam storage lifetime of 26 s obtained during the probing measurement was not entirely determined by the residual gas pressure but also by some accelerator related loss effect, then the correction for collisional quenching would be slightly smaller giving a shorter lifetime. Similarly, for the optical pumping measurement, if there is a small contribution from beam loss (not related to vacuum conditions) not included in the analysis, a slightly longer lifetime would be obtained.

Table 4. Comparison between the present results and previous experimental and theoretical results for radiative lifetimes of the metastable $4d\ ^2D$ levels in Sr^+. All values are given in ms.

Experimental	$4d\ ^2D_{3/2}$	$4d\ ^2D_{5/2}$
Gerz *et al.* [19]	395 ± 38	345 ± 33
Madej and Sankey [20]		372 ± 25
Barwood *et al.* [49]		347 ± 33
This work, laser probing	455 ± 29	408 ± 22
This work, optical pumping	435 ± 4	
Theory		
Warner [27]	257	209
Guet and Johnson [26]	454	405
Poirier [28]	441	396
This work	422	384

5 Discussion

There are two earlier experiments devoted to the determination of metastable lifetimes in Sr^+. The first was performed by Gerz *et al.* [19] in a r.f. quadrupole trap. The experimental method was similar to our measurement utilizing optical pumping, *i.e.* the d levels were populated through laser excitation of the resonance $5s$–$5p$ transition and the intensity decay of the E2 $5s$–$4d$ transitions was observed directly. Madej and Sankey [20] used, instead of a cloud of ions, only one single laser cooled strontium ion and by a measurement of the length of the dark periods obtained as the ion was kicked into the $4d\ ^2D_{5/2}$ and lost from the laser cooling cycle. The latter method should in principle be more accurate since apparent lifetime shortening due to loss of particles is avoided. Barwood *et al.* have worked on the strontium ion in order to establish methods for obtaining more accurate frequency standards (see *e.g.* Refs. [49,50]). In this context they mention a lifetime measurement they did on the $4d\ ^2D_{5/2}$ level in an ion trap. Their value is equal to the value obtained by Gerz *et al.* As can be seen from Table 4, our experimental values are systematically slightly longer than previous measurements. Our new calculations, as well as the calculations by Guet and Johnson [26] and by Poirier [28], favor slightly longer lifetimes as obtained in the present experiment. According to Poirier [28], the values obtained by Warner [27] should presumably be multiplied by 2, which then also would support longer lifetimes.

The homologous metastable $3d$ levels in Ca^+ have been thoroughly investigated experimentally as well as theoretically [51]. Also in this case our experimental results [29] obtained by the laser probing technique favored slightly longer lifetimes than obtained in most of the trap measurements. Here it was interesting to note that for an experiment done with one single laser cooled calcium ion, the obtained lifetime was significantly shorter [52]. Very recently, Block *et al.* [53] found an explanation for the shorter lifetimes. They showed that the measured lifetime was depending on the laser power of the repumping cooling laser ($4d\ ^2D_{3/2}$–$5p\ ^2P^0_{1/2}$) although its frequency

was far off resonance from the transition that involves the $3d\ ^2D_{5/2}$ level. They varied the laser power and extrapolated to zero intensity to find a lifetime unaffected by this quenching effect. They obtained a value close to our longer lifetime [29]. It is, of course, a general problem for lifetime measurements of long-lived metastable states, that there could be a number of different effects connected to the experimental situation that may cause quenching of the levels.

We have also calculated the lifetimes of a great number of excited levels, which can decay by allowed transitions. The HFR lifetime values calculated along the Rydberg series up to $n = 10$ are presented in Table 2 where they are compared with previous theoretical and experimental results. All the lifetimes are expressed in ns except for the metastable $4d$ levels (ms).

The physical model adopted for the present calculations can be further tested by comparing the HFR lifetime results with those obtained experimentally for $5p\ ^2P^0$ and $4f\ ^2F^0$ levels and, particularly, with the fast-beam-laser measurements of Pinnington *et al.* [25] which are expected to be very accurate. It is seen from Table 2 that the agreement is satisfactory, the theory leading, however, to lifetimes results systematically larger than the experiment, the differences being however rather small (in fact they range in between 2.6 and 8.7%). The lifetimes of the $5p\ ^2P^0$ levels have also been calculated by Guet and Johnson [26] and by Poirier [28] yielding slightly more accurate results.

6 Conclusions

We have shown that a stored fast ion beam excited with laser light could yield accurate experimental lifetime values, very competitive to what is presently achieved with ion traps. The present investigation has been focussed on the $4d\ ^2D_{3/2,5/2}$ in Sr^+, the latter of which has been selected as a candidate for a new more accurate frequency standard in the optical region. We also show that relativistically corrected Hartree-Fock calculation with inclusion of core polarization give accurate results for singly charged strontium. The comparison of the different sets of data available, including the experimental measurements of the present work, shows that the HFR lifetime values are probably accurate within a few (< 5) percent for most of the levels considered including the long lived metastable ones. In addition, a main advantage of the HFR approach, in comparison with the other theoretical methods quoted in this paper, is that predictions of lifetime values have been obtained for a large number of levels (see Tab. 2) with a reasonable computational effort.

We are grateful to the technical staff of the Manne Siegbahn Laboratory for excellent support during the measurements. Technical development of a tailored frequency doubling crystal was successfully performed by Håkan Karlsson and Fredrik Laurell at the Royal Institute of Technology in Stockholm. We are also obliged to them for lending us the standing-wave Ti:sapphire laser for the infra-red excitation. We are also grateful to Lars-Erik Berg from whom we borrowed equipment for the experiment. This project was supported by the Swedish Natural Science Research Council (NFR). EB is Research Director of the Belgian National Fund for Scientific Research (FNRS). Financial support from this organization is acknowledged. EB, AS and XT have very much appreciated the warm hospitality of the Manne Siegbahn Laboratory during their stays in Stockholm.

References

1. H. Dehmelt, IEEE Trans. Instrum. Meas. **31**, 83 (1982).
2. *Procès-Verbaux des Comités International des Poids et Mesures* (BIPM, Svres, France, 1998), Vol. 65, pp. 63-71.
3. J.E. Bernard, L. Marmet, A.A. Madej, Opt. Commun. **150**, 170 (1998).
4. J.E. Bernard, A.A. Madej, L. Marmet, B.G. Whitford, K.J. Siemsen, S. Cundy, Phys. Rev. Lett. **82**, 3228 (1999).
5. J.I. Cirac, P. Zoller, Phys. Rev. Lett. **74**, 4091 (1995).
6. Ch. Roos, Th. Zeiger, H. Rohde, H.C. Nägerl, J. Escher, D. Leibfried, F. Schmidt-Kaler, R. Blatt, Phys. Rev. Lett. **83**, 4713 (1999).
7. C. Jaschek, M. Jaschek, *The behavior of Chemical Elements in Stars* (Cambridge University Press, 1995).
8. A.H. Joy, Ap. J. **102**, 168 (1945).
9. K.Kodaira, M. Takada, Ann. Tokyo Obs. Sec. Ser. **17**, 79 (1978).
10. M.A. Smith, Ap. J. Suppl. **25**, 277 (1973); M.A. Smith, Ap. J. **189**, 101 (1974).
11. D.L. Lambert, in *Cool Stars with Excesses of Heavy Elements*, edited by M. Jaschek, P.C. Keenan (Reidel, 1985).
12. V.V. Smith, D.L. Lambert, Ap. J. **311**, 843 (1986).
13. J.F. Dominy, Ap. J. Suppl. **55**, 27 (1984).
14. C.E. Moore, M.G.J. Minnaert, J. Houtgast, NBS Monograph **61** (1966).
15. R.E. Luck, H.E. Bond, Ap. J. **292**, 559 (1985).
16. T. Brage, G.M. Wahlgren, S.G. Johansson, D.S. Leckrone, C.R. Proffitt, Ap. J. **496**, 1051 (1998).
17. T. Zethson, H. Hartman, S. Johansson, T.R. Gull, K. Davidson, K. Ishibashi, Astron. Astrophys. (submitted).
18. C.E. Moore, *Atomic Energy* Levels (Nat. Bur. Stand., Circular 467, Washington D.C., 1958), Vol. II.
19. Ch. Gerz, Th. Hilberath, G. Werth, Z. Phys. D **5**, 97 (1987).
20. A.A. Madej, J.D. Sankey, Opt. Lett. **15**, 634 (1990).
21. F.H.K. Rambow, L.D. Schearer, Phys. Rev. A **14**, 1735 (1976).
22. F.M. Kelly, T.K. Koh, M.S. Mathur, Can. J. Phys. **52**, 1666 (1974).
23. F.M. Kelly, T.K. Koh, M.S. Mathur, Can. J. Phys. **52**, 1438 (1974).
24. P. Kuske, N. Kirchner, W. Wittmann, H.J. Andrä, D. Kaiser, Phys. Lett. A **64**, 377 (1978).
25. E.H. Pinnington, R.W. Berends, M. Lumsden, J. Phys. B **28**, 2095 (1995).
26. C. Guet, W.R. Johnson, Phys. Rev. A **44**, 1531 (1991).
27. B. Warner, Mon. Not. Roy. Astron. Soc. **139**, 115 (1968).
28. M. Poirier, Z. Phys. D **25**, 117 (1993).
29. J. Lidberg, A. Al-Khalili, L.O. Norlin, P. Royen, X. Tordoir, S. Mannervik, J. Phys. B **32**, 757 (1999).
30. R.D. Cowan, *The Theory of Atomic Structure and Spectra* (Univ. of California Press, 1981).
31. R.D. Cowan, D.C. Griffin, JOSA **66**, 1010 (1976).

32. G.H. Newsom, S. O'Connor, R.C.M. Learner, J. Phys. B **6**, 2162 (1973).
33. J. Migdalek, W.E. Baylis, J. Q.S.R.T. **22**, 127 (1979).
34. E. Biémont, J.-F. Dutrieux, I. Martin, P. Quinet, J. Phys. B **31**, 3321 (1998).
35. E. Biémont, P. Quinet, V. van Renterghem, J. Phys. B **31**, 5301 (1998).
36. S. Fraga, J. Karwowski, K.M.A. Saxena, *Handbook of Atomic Data* (Elsevier, Amsterdam, 1976).
37. R.D. Knight, M.H. Prior, Phys. Rev. A **21**, 179 (1980).
38. T. Andersen, Nucl. Instrum. Meth. Phys. Res. B **123**, 508 (1997).
39. H.T. Schmidt, P. Forck, M. Grieser, D. Habs, J. Kenntner, G. Miersch, R. Repnow, U. Schramm, T. Schüssler, D. Schwalm, A. Wolf, Phys. Rev. Lett. **72**, 1616 (1994).
40. J. Doerfert, E. Träbert, A. Wolf, D. Schwalm, O. Uwira, Phys. Rev. Lett. **78**, 4355 (1997).
41. S. Mannervik, L. Broström, J. Lidberg, L.O. Norlin, P. Royen, Phys. Rev. Lett. **76**, 3675 (1996).
42. J. Lidberg, A. Al-Khalili, L.O. Norlin, P. Royen, X. Tordoir, S. Mannervik, Nucl. Instrum. Meth. B **152**, 157 (1999).
43. K. Abrahamsson, G. Andler, L. Bagge, E. Beebe, P. Carlé, H. Danared, S. Egnell, K. Ehrnstén, M. Engström, C.J. Herrlander, J. Hilke, J. Jeansson, A. Källberg, S. Leontein, L. Liljeby, A. Nilsson, A. Paal, K.-G. Rensfelt, U. Rosengård, A. Simonsson, A. Soltan, J. Starker, M. af Ugglas, A. Filevich, Nucl. Instrum. Meth. Phys. Res. B **79**, 268 (1993).
44. S. Mannervik, J. Lidberg, L.O. Norlin, P. Royen, A. Schmitt, W. Shi, X. Tordoir, Phys. Rev. Lett. **83**, 698 (1999).
45. S. Mannervik, J. Lidberg, L.O. Norlin, P. Royen, Phys. Rev. A **56**, R1075 (1997).
46. H. Karlsson H., F. Laurell, Appl. Phys. Lett. **71**, 3474 (1997).
47. A. Kerek, W. Klamra, L.O. Norlin, D. Novák, S. Westman, J. Lidberg, S. Mannervik, *Proceedings of the 6th European Particle Accelerator Conference* (EPAC98), Institute of Physics Publishing, Bristol and Philadelphia, 1998, p. 1577.
48. L. Bagge, H. Danared, private communication.
49. G.P. Barwood, C.S. Edwards, P. Gill, G. Huang, H. Klein, W.R.C. Rowley, IEEE Trans. Instrum. Meas. **44**, 117 (1995).
50. G.P. Barwood, G. Huang, H.A. Klein, P. Gill, R.B.M. Clarke, Phys. Rev. A **59**, R3178 (1999).
51. E. Biémont, C.J. Zeippen, Comm. At. Mol. Phys. **33**, 29 (1996).
52. G. Ritter, U. Eichmann, J. Phys. B **30**, L141 (1997).
53. M. Block, O. Rehm, P. Seibert, G. Werth, Eur. Phys. J. D **7**, 461 (1999).
54. W.W. Smith, A. Gallagher, Phys. Rev. **145**, 26 (1966).
55. A. Lindgard, S.E. Nielsen, At. Data Nucl. Data Tab. **19**, 533 (1977).
56. A. Gallagher, Phys. Rev. **157**, 24 (1967).